

PACS numbers: 42.55.Wd; 42.60.By; 42.81.Bm
DOI: 10.1070/QE2015v045n05ABEH015762

Fibre amplifier based on an ytterbium-doped active tapered fibre for the generation of megawatt peak power ultrashort optical pulses

M.Yu. Koptev, E.A. Anashkina, K.K. Bobkov, M.E. Likhachev, A.E. Levchenko, S.S. Aleshkina, S.L. Semjonov, A.N. Denisov, M.M. Bubnov, D.S. Lipatov, A.Yu. Laptev, A.N. Gur'yanov, A.V. Andrianov, S.V. Muravyev, A.V. Kim

Abstract. **We report a new ytterbium-doped active tapered fibre used in the output amplifier stage of a fibre laser system for the generation of megawatt peak power ultrashort pulses in the microjoule energy range. The tapered fibre is single-mode at its input end (core and cladding diameters of 10 and 80 μm) and multimode at its output end (diameters of 45 and 430 μm), but ultrashort pulses are amplified in a quasi-single-mode regime. Using a hybrid Er/Yb fibre system comprising an erbium master oscillator and amplifier at a wavelength near 1.5 μm, a nonlinear wavelength converter to the 1 μm range and a three-stage ytterbium-doped fibre amplifier, we obtained pulses of 1 μJ energy and 7 ps duration, which were then compressed by a grating-pair dispersion compressor with 60% efficiency to a 130 fs duration, approaching the transform-limited pulse duration. The present experimental data agree well with numerical simulation results for pulse amplification in the three-stage amplifier.**

Keywords: *ytterbium-doped tapered fibre, Er/Yb fibre laser system, ultrashort pulse amplification.*

1. Introduction

The rapid growth of the output power of pulsed and cw ytterbium-doped fibre lasers is imposing ever more stringent requirements for the fibres to be used in such lasers, especially as to the ability to raise their threshold for nonlinear effects. Standard single-mode ytterbium-doped fibres have a relatively low threshold for nonlinear effects, because of the relatively small size of their core (6–10 μm) and the large fibre length (more than 10 m in a number of cases). The problem of raising the threshold for nonlinear effects is particularly critical in the case of pulsed fibre systems, where the peak power reaches hundreds of kilowatts, approaching the megawatt level. The simplest and most obvious way to raise the threshold for nonlinear effects is to increase the core diameter and, hence, the fundamental mode field diameter. However, with existing fibre designs, this leads to two problems: the fibre switches to multimode operation (degrading the output beam quality) and acquires very high bend loss sensitivity (so that only almost straight fibres can be used, which rules out the possibility of producing compact designs).

The purpose of this work was to develop a new approach based on the use of so-called tapered fibre, which allows one to reach large mode field diameters and, at the same time, maintain acceptable bend loss sensitivity. In this study, optimising the parameters of such fibre and using it in the final stage of an ytterbium-doped fibre amplifier of chirped picosecond pulses allowed us to obtain the highest output peak power among all-fibre systems and approach the record level of microstructured rod-type fibres.

2. Existing types of large mode field diameter fibre

In standard step-index fibres, one can increase the core diameter to 15–20 μm, maintaining single-mode propagation of light at a wavelength of 1080 nm (at a numerical aperture of the fibre NA = 0.04–0.05), but the bend loss sensitivity of such fibres will be unacceptably high. This problem can be obviated by using few-mode operation. The core diameter of a step-index fibre can then be increased to 25–30 μm, and its higher order modes can be suppressed by winding it onto a spool of certain radius [1, 2]. At the same time, further increasing the core diameter leads to significant beam quality degradation ($M^2 \sim 1.4$ and 1.9 at core diameters of 40 [3] and 50 μm [2], respectively) even at the optimal fibre bend diameter.

To date, the largest mode field diameter has been obtained in microstructured fibres (MSFs). In such fibres, the core contains an active dopant and is surrounded by a two-dimensional (2D) array of air-filled capillaries, which ensure effective fundamental mode confinement and higher order mode filtration. In MSFs, single-mode propagation can be maintained at core diameters of up to 40 μm [4], in combination with reasonable bend loss sensitivity. Further increase in core diameter is possible in the case of differential mode amplifica-

M.Yu. Koptev, E.A. Anashkina, A.V. Andrianov, S.V. Muravyev, A.V. Kim Institute of Applied Physics, Russian Academy of Sciences, ul. Ul'yanova 46, 603950 Nizhnii Novgorod, Russia; N.I. Lobachevsky State University of Nizhnii Novgorod, prosp. Gagarina 23, 603950 Nizhnii Novgorod, Russia; e-mail: elena.anashkina@gmail.com;
K.K. Bobkov, M.E. Likhachev, A.E. Levchenko, S.S. Aleshkina, S.L. Semjonov, A.N. Denisov, M.M. Bubnov Fiber Optics Research Center, Russian Academy of Sciences, ul. Vavilova 38, 119333 Moscow, Russia;
D.S. Lipatov N.I. Lobachevsky State University of Nizhnii Novgorod, prosp. Gagarina 23, 603950 Nizhnii Novgorod, Russia; G.G. Devyatykh Institute of Chemistry of High-Purity Substances, Russian Academy of Sciences, ul. Tropinina 49, 603950 Nizhnii Novgorod, Russia;
A.Yu. Laptev, A.N. Gur'yanov G.G. Devyatykh Institute of Chemistry of High-Purity Substances, Russian Academy of Sciences, ul. Tropinina 49, 603950 Nizhnii Novgorod, Russia

Received 29 January 2015
Kvantovaya Elektronika **45** (5) 443–450 (2015)
Translated by O.M. Tsarev

tion, where the MSF structure and ytterbium oxide doping region are chosen so that the fundamental mode has the largest gain coefficient. This approach made it possible to fabricate an ytterbium-doped MSF with a core diameter above 100 μm and to obtain the best results so far: 1 MW of peak power directly in a fibre amplifier and 3.8 GW after the compression of chirped pulses with diffraction gratings [5].

It is important to point out that the MSFs have a number of serious drawbacks. Note, first of all, that they are difficult to fabricate. In particular, one has to maintain a predetermined pressure in their holes during fibre drawing. As a result, fibres with tailored parameters are difficult to produce and, accordingly, are expensive. No less important is that light is difficult to couple into and outcouple from MSFs: they can only be combined with conventional fibres using 3D components (lenses and three-axis positioning systems). Moreover, because of their increased bend loss sensitivity, they are produced in the form of rod-type fibres 0.5 to 2 mm in diameter, which should be absolutely straight. Thus, the use of MSFs eliminates the key advantages of fibre lasers: compact design (microstructured rod-type fibres are typically 1.5–2 m in length), reliability (light coupling/decoupling elements may be misaligned) and low cost in comparison with solid-state lasers.

As a consequence, considerable attention is currently paid to a search for alternative waveguide structures with a large mode field diameter but reduced bend loss sensitivity. A separate important issue is the ability to integrate optical fibre into all-fibre laser designs. Such structures include leakage channel fibres [6], higher order mode fibres [7], step-index fibres with a microstructured cladding that suppresses higher order modes [8], helical-core fibres [9], so-called chirally coupled core (3C) fibres [10], photonic band gap fibres [11, 12] and others. Despite the extensive work along these lines, in none of the above cases was the level of MSFs approached. In particular, the peak power directly at the amplifier output does not exceed a few tens of kilowatts, which is almost two orders of magnitude below the level reached with microstructured rod-type fibres.

Relatively recently, a novel approach has been proposed for producing high nonlinear threshold amplifiers, which takes advantage of tapered fibres [13, 14]. Central to this approach is the use of an active fibre in which the core and cladding diameters vary monotonically along its length. Seed light is coupled into the fibre through its thin, single-mode end, and a dichroic mirror is used to outcouple the amplified light and launch pump radiation through the thick fibre end. As shown by Stacey et al. [15] and Jung et al. [16], in the case of an adiabatic variation in core diameter the excitation of the fundamental mode at the thin end of a tapered fibre does not cause conversion of this mode to higher order modes as the light propagates along the fibre. Thus, when the core diameter increases sufficiently slowly, the tapered fibre basically behaves as single-mode fibre even though the core diameter (and the fundamental mode field size) at its thick end may exceed the single-mode core diameter many times. Light propagating through the thin part of the tapered fibre (with a small mode field diameter) then has low intensity, whereas the amplified light propagates through the large core diameter region. It should also be emphasised that such fibres have rather low bend loss sensitivity and can be integrated into an all-fibre system: the thin end of a tapered fibre can readily be fusion-spliced to the output of a preamplifier. At the same time, despite the great potential offered by this approach, the results obtained using it are far from the level reached with MSFs. This is mainly due to the relatively long length of the transition section between the thin and thick ends (several meters); the relatively weak pump absorption from the cladding because of the small ratio of the core and cladding diameters; and the large numerical aperture (NA > 0.11), which makes it impossible to obtain a large mode field diameter even at a relatively large core diameter (~40 μm) [13, 14].

3. Tapered fibre design optimisation

3.1. Core composition

To maximise the threshold for nonlinear effects in an amplifier, it is important not only to increase the mode field diameter but also to raise the ytterbium concentration in the fibre core. The latter determines the maximum gain per unit length of the fibre and, hence, the minimum fibre length necessary for making an amplifier. A major problem related to the development of large mode field diameter fibres is that, in most of the waveguide structures proposed to date, the refractive index (RI) of the core should be close or even equal to that of undoped silica glass. At the same time, the addition of 1–2 wt% ytterbium oxide to the glass network increases the RI of the core by 0.001–0.002. An even more serious problem is the low ytterbium oxide solubility in silica glass (which leads to an increase in background loss and photodarkening). This requires additional doping with alumina, which causes an even more appreciable increase in the RI of the core. This issue can be partially resolved by additional doping with fluorine, which reduces the RI of the core. However, in this case too, the limiting ytterbium oxide concentration that can be reached in the core of large mode field diameter fibres is substantially lower (typically by three to four times) than that characteristic of standard ytterbium-doped fibres.

One solution to this problem is to use a phosphoaluminosilicate glass matrix developed by us for doping with rare-earth elements. Basic to this approach is a well-known effect: the formation of the $AlPO_4$ compound on the addition of equimolar amounts of alumina and phosphorus oxide to silica glass [17]. This compound is similar in properties (structure, RI, density and others) to undoped silica glass [17, 18]. At the same time, the solubility of the rare-earth elements in SiO_2–$AlPO_4$ glass was shown to be several orders of magnitude higher [18]. It is the use of such a glass matrix that enabled us to reach a record high ytterbium oxide concentration (about 2 wt%) in a fibre with a core–cladding index difference as small as 0.002 [19]. Another advantage of the approach in question is almost complete suppression of the photodarkening effect [19]. It is such a glass matrix that was used in this study for the fabrication of the core of tapered fibre.

3.2. Fibre design

In addition to the ytterbium oxide concentration, there is another, no less important factor: the ratio of the core and cladding diameters in the active fibre. This factor determines the rate of pump absorption from the cladding and, hence, the effective amplifier length. The maximum core diameter of a tapered fibre is determined by the constraint of single-modedness at the thin fibre end. In our case, single-mode

operation was ensured by a core diameter of 10 μm. The minimum cladding diameter is 80 μm, as determined by the condition of employing standard fusion splicing equipment for joining the tapered fibre to the preamplifier stage of a laser. Note that the thick end diameter of typical tapered fibres with a tapering ratio of 5–6 reaches 0.5 mm even when the diameter of their thin end is 80 μm. This poses serious problems in preparing quality end facets: the thick fibre end should be angle-cleaved to avoid back reflection, and the quality of the cleave should be high enough for multimode pump to be coupled into the fibre. As a rule, highly specialised, expensive fibre cleavers are needed to produce high-quality end facets of thick fibres. Moreover, in the fabrication of polarisation-maintaining fibres it is desirable to be able to control the angle cleave orientation with respect to the stress rods, which is a nontrivial issue even when specialised fibre cleavers are used. This issue can be resolved by using double-clad all-glass fibres with highly fluorinated silica glass instead of a reflective polymer. This allows one to reach the desired quality of the output fibre end face by merely gluing the fibre into an adapter and then polishing the adapter by a standard procedure. In this study, we used a double-clad all-silica fibre. Figure 1a shows a micrograph of a cross section of the tapered fibre.

Note that the ratio of the diameters of the fluorinated and undoped silica claddings in the fibre under consideration was about 1.2. As a result, the cross-sectional area of the inner (undoped silica) cladding was a factor of 1.5 smaller than that in silica–polymer fibres [at a fixed outer diameter of the thin end (80 μm) and a fixed single-mode core diameter (10 μm)], which led to a proportional increase in pump absorption from the cladding.

The above improvements in the tapered fibre design ensured a record strong pump absorption from the cladding, about 5 dB m^{-1} at a wavelength of 915 nm and about 20 dB m^{-1} at 976 nm (Fig. 1b), which is about 20 times that in tapered fibres reported previously [13, 14].

3.3. Tapered fibre fabrication

Modern tapered fibre fabrication techniques allow one to produce fibres with tapering lengths from several centimetres to several metres, with rather accurate control over the diameter profile along the fibre and large tapering ratios [20]. At the same time, such techniques are rather expensive and require considerable effort and unconventional equipment. A simpler, less expensive and more efficient approach is to produce tapered fibres directly during the fibre drawing process by varying the drawing speed. The method was developed as early as 1991 at the Fiber Optics Research Center (FORC), Russian Academy of Sciences [21]. It is worth noting that drawing parameters (including the process temperature, fibre draw speed and preform feed rate) have a rather slow effect on the fibre diameter in the drawing process, which allowed this method to be used for drawing relatively long tapered fibres: from 10 m to several kilometres. It seems likely that it is for this reason that, in previous studies where a similar method was used [13, 14], the length of tapered fibres (determined, in fact, by the rate of change in fibre diameter during the drawing process) exceeded several metres, which is unacceptable in the fabrication of tapered fibres with a high threshold for nonlinear effects.

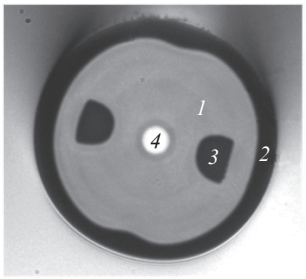

a

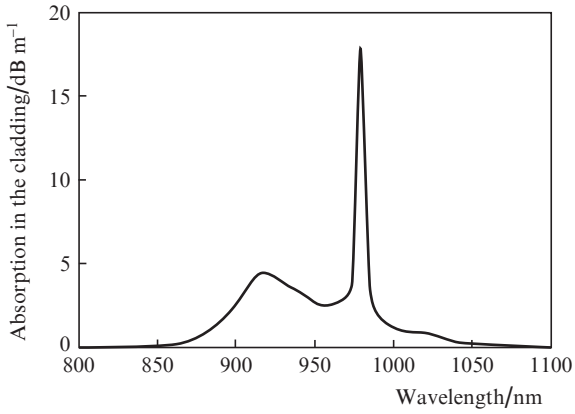

b

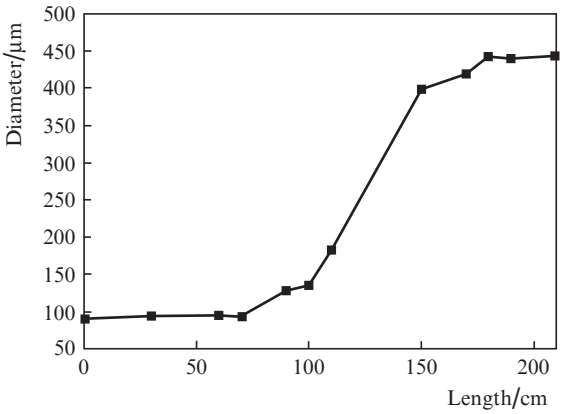

c

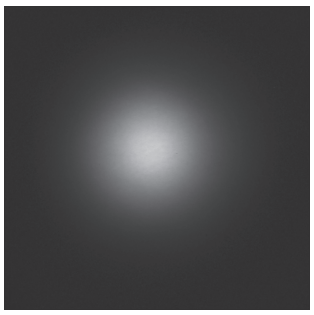

d

Figure 1. (a) Cross section of tapered fibre: (*1*) undoped silica cladding, (*2*) fluorinated silica cladding, (*3*) borosilicate stress rods, (*4*) ytterbium oxide-doped phosphoaluminosilicate core; (b) absorption spectrum of the tapered fibre for pump light propagating in the cladding; (c) longitudinal diameter profile of the tapered fibre; (d) intensity distribution at the output of the tapered fibre.

The problem of producing short (1 m or shorter) tapered fibres in the fibre drawing process was resolved about 15 years ago at FORC [22]. To this end, all the drawing parameters were kept unchanged and the fibre diameter was varied by changing the flow rate of an inert gas passing through a furnace. The inert gas (as a rule, argon) transfers heat from a heating element to the fibre preform, and changes in gas flow rate lead to sharp changes in the temperature of the glob of molten glass, which enables very sharp changes in fibre diameter (the tapering length can be as short as a few tens of centimetres), including periodic changes according to a preset law.

To date, the technique for varying the fibre diameter during the fibre drawing process has been updated and automated, which allows us to draw tapered fibres a few tens of centimetres to several kilometres in length, with accurate control over the diameter profile along the fibre. Periodic variations in fibre drawing conditions allow series of identical tapered fibres to be drawn in drawing cycle (with scatter in their parameters from sample to sample within a few percent). The number of cycles, equal to the number of tapered fibres thus produced, is only limited by the preform size. It should be emphasised that the method under consideration can be used, without any modifications, to draw both passive and active tapered fibres. Figure 1c shows the outer diameter profile along the length of an ytterbium-doped tapered fibre produced by drawing at FORC. The tapering length was slightly above 0.5 m, which is almost one order of magnitude smaller than that in tapered fibres reported previously [13, 14]. The core and cladding diameters in the tapered fibre were 10 and 80 μm at the thin end and 50 and 430 μm at the thick end.

It should be especially emphasised that, even though formally the output end of the tapered fibre is multimode (normalised frequency is $V \sim 11$), assessment of the mode composition demonstrates that, when light propagates from the thin fibre end to the thick one, higher order modes are not excited and the output mode field has a nearly Gaussian shape. The shape of the mode is insensitive to variations in excitation conditions at the input, single-mode end of the fibre and to fibre bending to a diameter of 20 cm, indicating that there is single-mode light propagation. Figure 1d shows a photograph of the intensity distribution at the output of the fibre operating in amplification mode.

4. Ultrashort pulse amplification in the ytterbium-doped tapered fibre

The tapered fibre was used in experiments on ultrashort pulse amplification to megawatt peak powers. Figure 2 shows a schematic of the experimental setup. Its key component is a femtosecond ring-cavity erbium-doped fibre laser diode-pumped at a wavelength of 975 nm. The laser is passively mode-locked via nonlinear rotation of the polarisation ellipse of a femtosecond pulse based on the optical Kerr effect. The master oscillator generates 230-fs pulses at a repetition rate of 50 MHz and a wavelength of 1.56 μm [23]. The scheme also includes a fibre Faraday isolator and a two-stage erbium-doped fibre amplifier, after which the ultrashort 1.5-μm pulses with ~100 mW of average power are converted to 1-μm pulses with about 10% efficiency. As a nonlinear optical converter, we use a short (~10 cm) piece of dispersion-shifted fibre (DSF). The upconversion is due to spectral broadening upon soliton pulse compression in the low anomalous dispersion region and linear wave generation in the normal dispersion region under phase-matching conditions [23–25]. Note that ultrashort 1-μm pulses obtained in such configurations were used previously as a seed for ytterbium fibre amplifiers with a constant fundamental mode diameter [23, 25, 26].

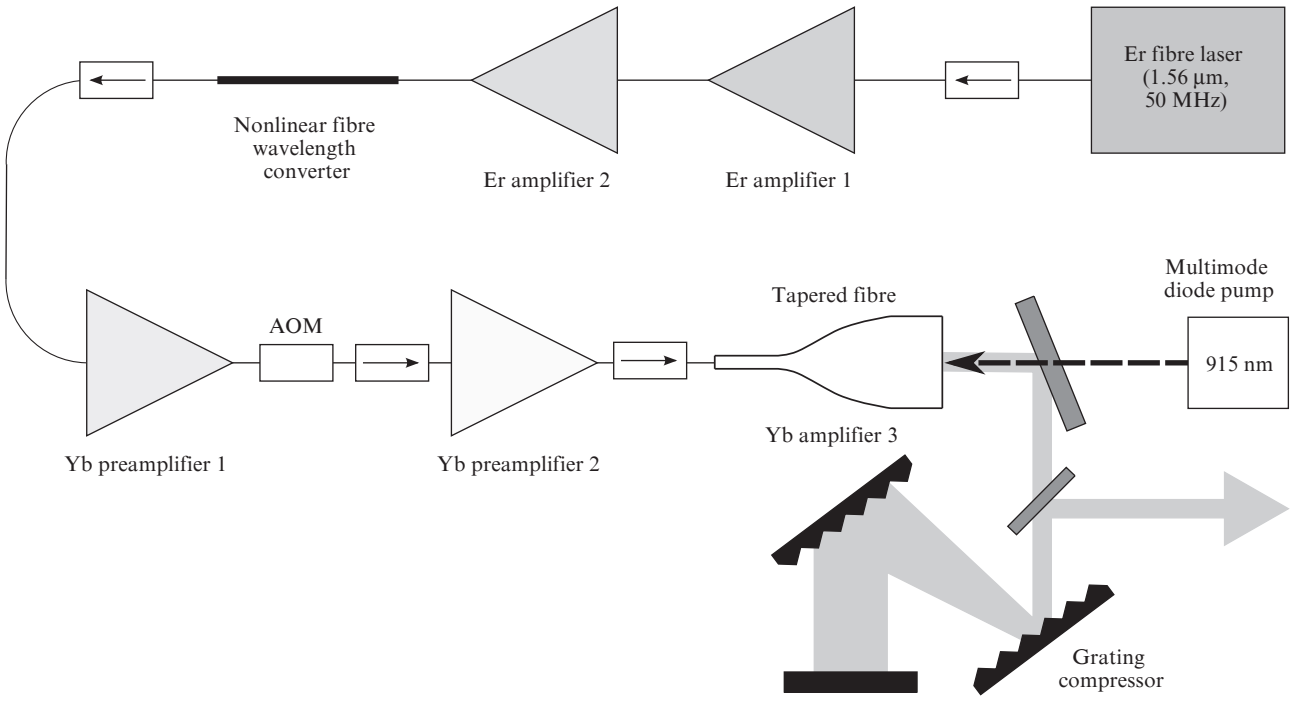

Figure 2. Schematic of the experimental setup for the generation of megawatt peak power ultrashort pulses.

After the DSF, there are two ytterbium-doped fibre power preamplifiers, with an acousto-optic modulator (AOM) in between for reducing the pulse repetition rate to 1 MHz. The first ytterbium fibre preamplifier uses a non-polarisation-maintaining fibre, and the second uses a polarisation-maintaining active fibre. The AOM is needed to reduce the average pump power in the output stage of the tapered amplifier for obtaining microjoule pulses. After the second ytterbium fibre preamplifier, the average signal power is ~10 mW, which corresponds to a pulse energy of ~10 nJ. Next, there is an amplifier based on a polarisation-maintaining ytterbium-doped tapered fibre. The pulses at its output have a 1-μJ energy and 7-ps duration. Here and in what follows, pulses were characterised using the frequency-resolved optical gating (FROG) technique. Figure 3a shows the spectrum of the signal and the spectral phase of FROG-retrieved pulses. The time-domain pulse intensity distribution is presented in Fig. 3b. The peak power directly in the tapered fibre-based output amplifier stage reached 100 kW, which is a record high level for all-fibre amplifiers.

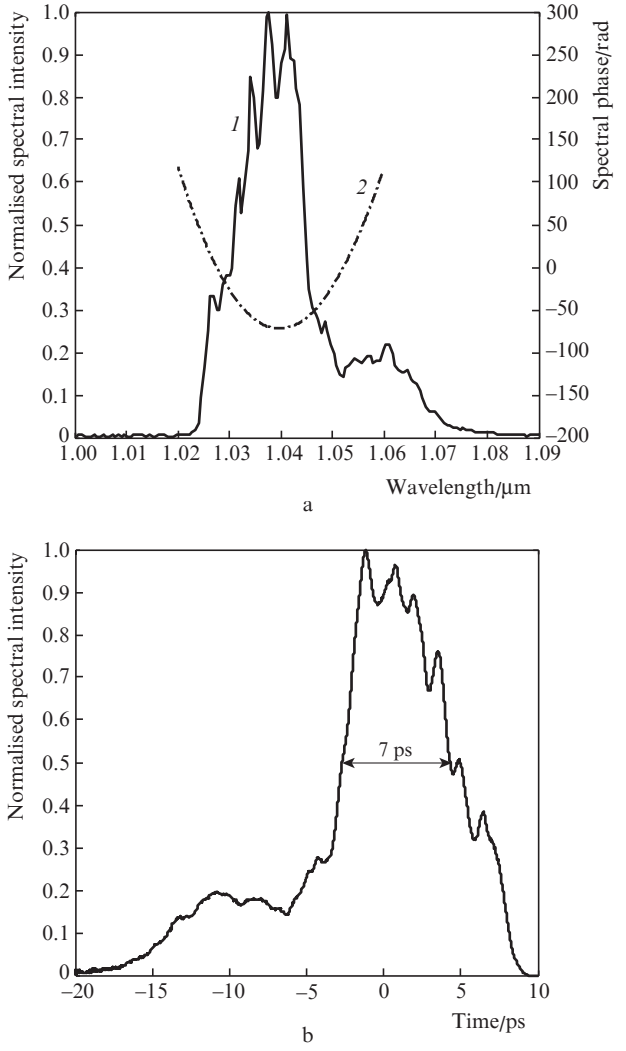

Figure 3. (a) (*1*) Spectrum of the signal at the output of the ytterbium-doped tapered fibre and (*2*) FROG-retrieved spectral phase; (b) FROG-retrieved time-domain signal intensity distribution.

The microjoule pulses were compressed using a grating-pair dispersion compressor. At optimal compressor parameters, we obtained 130-fs pulses with a 60% compressor efficiency. Figure 4a shows an independently measured spectrum of the signal and the spectral phase of FROG-retrieved pulses. The time-domain intensity distribution is presented in Fig. 4b. The inset in Fig. 4b shows an experimentally measured FROG trace. The time–bandwidth product is 0.48. The estimated peak power of FROG-retrieved pulses (with their real shape taken into account) is 2.5 MW. To calculate the peak power, the intensity distribution was integrated with respect to time and normalised to the total signal energy (600 nJ including the pedestal). Note that the pedestal in time domain is formed predominantly by long-wavelength (above 1.05 μm) spectral components, whereas the central peak has a rather good shape and an almost flat spectral phase.

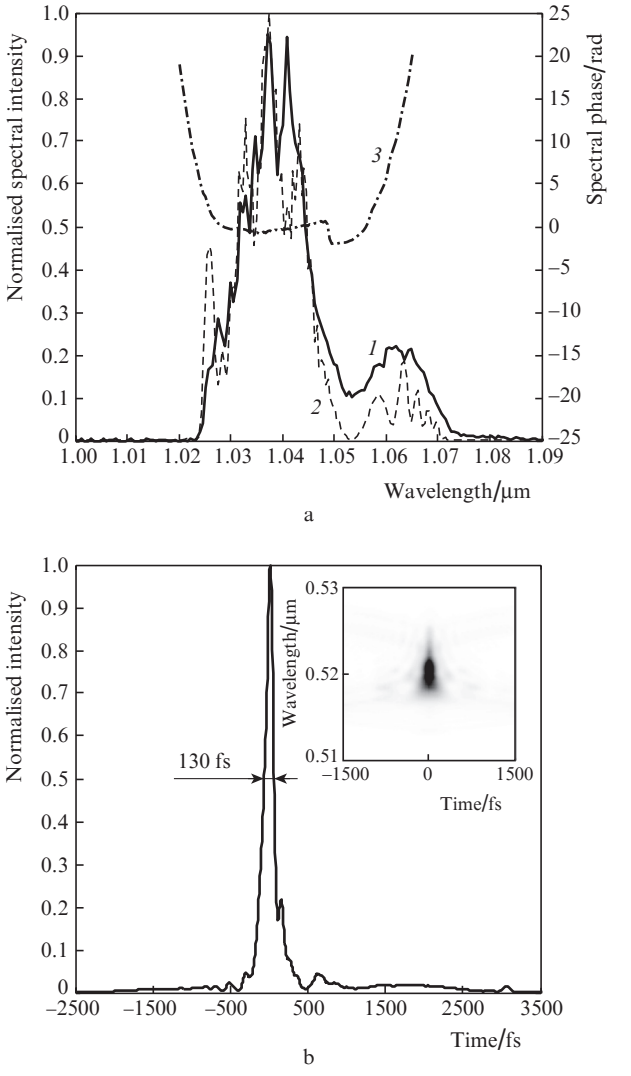

Figure 4. (a) Spectrum of the amplified compressed signal after a dispersion compressor: (*1*) measured with a spectrometer and (*2*) obtained for a FROG-retrieved pulse; (*3*) FROG-retrieved spectral phase; (b) FROG-retrieved time-domain signal intensity distribution; inset: experimentally measured FROG trace.

5. Numerical simulation of ultrashort pulse amplification in a three-stage ytterbium fibre amplifier

Using numerical simulation, we examined the amplification of transform-limited 70-fs Gaussian pulses of energy 200 pJ with a centre wavelength of 1.04 μm, propagating in all ytterbium-doped active fibres and in connecting passive fibres a total of ~5 m in length, with parameters corresponding to our experiments. The initial characteristics of the pulses corresponded to the signal immediately after the DSF. The spectrum of input pulses is shown in Fig. 5 by a dashed line.

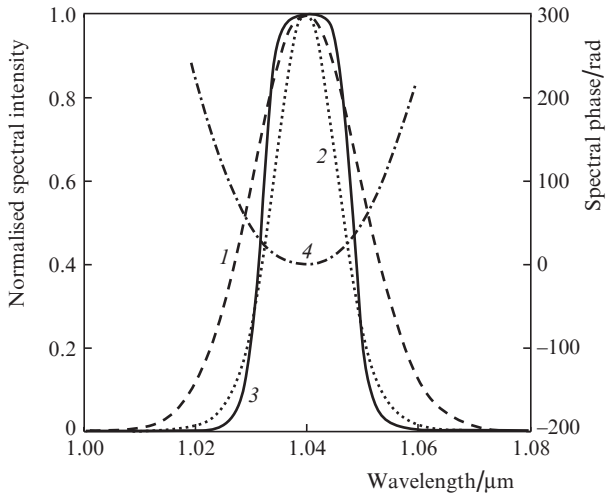

Figure 5. (*1*) Calculated spectrum of the signal at the input of the ytterbium fibre preamplifier 1, (*2*) spectrum of the signal after preamplifier 2 and (*3*) spectrum and (*4*) spectral phase of the signal at the tapered fibre output.

The spectral–temporal evolution of pulses in rare earth (ytterbium) doped active fibres was analysed in terms of a generalised nonlinear Schrödinger equation [27], which took into account not only Kerr and Raman nonlinearities and dispersion but also the homogeneously broadened gain band corresponding to the $^4F_{5/2} \rightarrow {}^4F_{7/2}$ laser transition (~1 μm wavelength) [28]:

$$\frac{\partial \tilde{A}(z,\omega)}{\partial z} + \frac{i\beta_{2j}(z)\omega^2}{2}\tilde{A}(z,\omega) + \frac{i\beta_{3j}(z)\omega^3}{6}\tilde{A}(z,\omega)$$
$$- i\gamma_j(z)\Big(1+\frac{\omega}{\omega_0}\Big)\hat{F}\Big[A(z,\tau)\int R(\tau-\eta)\,|A(z,\eta)|^2 d\eta\Big]$$
$$= G_j \exp(-\alpha_j z)\Big(\frac{1}{1+\omega^2 T_2^2} - \frac{i\omega T_2}{1+\omega^2 T_2^2}\Big)\tilde{A}(z,\omega), \qquad (1)$$

where $A(z,\tau)$ is the complex electric field envelope; the z-coordinate is measured along the fibre; ω is the angular frequency measured from the centre frequency ω_0; τ is the time in an accompanying frame; γ_j is the nonlinearity coefficient; β_{2j} and β_{3j} are the second- and third-order dispersion coefficients of the jth active fibre; $\hat{F}$ is the Fourier transform operator; $\tilde{A}(z,\omega) = \hat{F}[A(z,\tau)]$; $R(\tau)$ is the Raman response function [27]; T_2 is the phenomenological polarisation relaxation time; α_j is the unsaturated pump absorption coefficient (which is formally less than zero for the tapered fibre, because it is pumped by a counterpropagating beam, rather than by a copropagating beam as in the case of the first two preamplifiers); and G_j is a constant for the gain of the jth amplifier. For the first and second preamplifiers of length 1 and 2 m, respectively, with a constant core diameter, the coefficients γ, β_2 and β_3 are independent of z, whereas those of the output stage, made of a variable-diameter fibre, depend on z. To find the propagation constants β and transverse electric field structures of the fundamental modes of axisymmetric fibres of various diameters, we solved the problem of eigenvalues and eigenfunctions of the Helmholtz equation [29]. For the fundamental modes of the first two preamplifiers, we obtained $\gamma_{1,2} = 1\ W^{-1}\ km^{-1}$, $\beta_2 = 50\ ps^2\ km^{-1}$ and $\beta_3 = 0.05\ ps^3\ km^{-1}$. In estimating the nonlinearity coefficient of the tapered fibre, γ_3, at a wavelength of 1.04 μm, we used the diameters experimentally measured at various points (data points in Fig. 1c). In our calculations, we used a smoothed dependence of the nonlinearity coefficient on the length of the tapered fibre (Fig. 6).

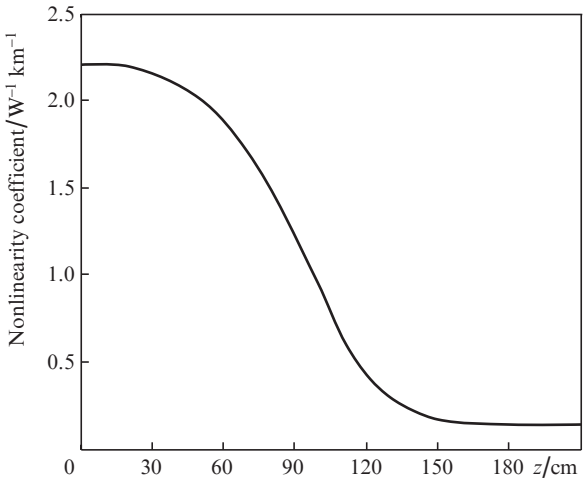

Figure 6. Nonlinearity coefficient vs. z-coordinate along the length of the ytterbium-doped tapered fibre.

Amplification was assumed to occur in the single-mode regime, which is justified by 3D modelling results for multimillijoule ytterbium fibre amplifiers [30]. As shown by Andrianov et al. [30], even when a fibre has various defects (bends, random core displacements and others) signal energy transfer to higher modes may be small.

Numerical modelling of Eqn (1) was performed using the pseudospectral, split-step Fourier method (SSFM) and fast Fourier transformation [27]. In modelling the nonlinear dynamics of ultrashort pulses in passive fibres, we also used the generalised nonlinear Schrödinger equation (1) with $G = 0$.

Figure 5 presents the numerical modelling results. In the first two amplifier stages, amplification is almost linear, and the pulse energy increases to 10 nJ at a pulse duration of 6.4 ps. The spectrum becomes narrower because the input spectrum is broader than the gain band. When pulses are ampli-

fied to an energy of 1 μJ, the effect of Kerr nonlinearity becomes significant. We observe self-phase modulation, which increases the bandwidth. The spectral shape differs rather markedly from Gaussian, approaching a rectangular shape. The pulse duration at the output of the tapered fibre is 6.8 ps. The duration of the corresponding transform-limited pulse is 120 fs, in good agreement with our experimental data. When the pulse is compressed to the transform limit with 60% efficiency (like in our experiments), the peak power reaches 4 MW, which exceeds the experimentally determined value of 2.5 MW, because in experiments there is some energy in the pulse pedestal, whereas in our calculations it was small in an ideal case. To raise the output energy, input pulses should be stretched to longer durations in order to minimise the effect of Kerr nonlinearity and linear phase distortions, which are rather difficult to compensate for using a dispersion compressor.

6. Conclusions

We have designed and investigated a new polarisation-maintaining ytterbium-doped tapered fibre for ultrashort pulse amplification to megawatt peak powers. The tapered fibre is single-mode at its input end (core and cladding diameters of 10 and 80 μm) and multimode at its output end (diameters of 45 and 430 μm), but ultrashort pulses are amplified in a quasi-single-mode regime. In the case of a counterpropagating multimode 915-nm pump beam, the fibre was employed as an output amplifier stage in a hybrid Er/Yb fibre system. We obtained 1.04 μm pulses of 1 μJ energy and 7 ps duration at a repetition rate of 1 MHz, which were then compressed by a grating-pair dispersion compressor with 60% efficiency to a 130 fs duration, approaching the transform-limited pulse duration. The shape of the pulses and their time-domain and spectral phases were measured using the FROG technique. The peak power of the compressed pulses was estimated at 2.5 MW. We performed numerical simulation of the propagation of ultrashort pulses in a three-stage ytterbium fibre amplifier and in passive fibres connecting the stages. Numerical calculations were made using a generalised nonlinear Schrödinger equation by the SSFM in combination with fast Fourier transformation. The obtained experimental data and numerical results agree well. It has been shown that, when 7-ps pulses are amplified in the tapered fibre to 1 μJ energy, the effect of Kerr nonlinearity is significant, so to raise the energy and peak power of the compressed pulses the input signal should be stretched to longer durations.

Acknowledgements. This research was supported by the Russian Foundation for Basic Research (Grant Nos 14-02-31645, 14-29-08217 and 15-32-20641), the RF President's Grants Council (State Support to Young Russian Scientists Programme, Grant No. MK-5947.2014.2), the Presidium of the Russian Academy of Sciences (Extreme Light Fields and Their Applications Programme) and the RF Ministry of Education and Science (Agreement No. 02.V.49.21.0003).

References

1. Koplow J.P., Kliner D.A.V., Goldberg L. *Opt. Lett*., **25**, 442 (2000).
2. Machewirth D., Khitrov V., Manyam U., Tankala K., Carter A., Abramczyk J., Farroni J., Guertin D., Jacobson N. *Proc. SPIE Int. Soc. Opt. Eng.*, **5335**, 140 (2004).
3. Jeong Y., Sahu J., Payne D., Nilsson J. *Opt. Express*, **12**, 6088 (2004).
4. Limpert J., Liem A., Reich M., Schreiber T., Nolte S., Zellmer H., Tünnermann A., Broeng J., Petersson A., Jakobsen C. *Opt. Express*, **12**, 1313 (2004).
5. Eidam T., Rothhardt J., Stutzki F., Jansen F., Hädrich S., Carstens H., Jauregui C., Limpert J., Tünnermann A. *Opt. Express*, **19**, 255 (2011).
6. Wong W.S., Peng X., McLaughlin J.M., Dong L. *Techn. Dig. Conf. on Lasers and Electro-Optics/Quantum Electronics and Laser Science and Photonic Applications Systems Technologies* (New York: OSA, 2005) paper CPDB10.
7. Ramachandran S., Nicholson J.W., Ghalmi S., Yan M.F., Wisk P., Monberg E., Dimarcello F.V. *Opt. Lett*., **31**, 1797 (2006).
8. Lavoute L., Roy P., Desfarges-Berthelemot A., Kermène V., Février S. *Opt. Express*, **14**, 2994 (2006).
9. Wang P., Cooper L.J., Sahu J.K., Clarkson W.A. *Opt. Lett*., **31**, 226 (2006).
10. Liu C.-H., Chang G., Litchinister N., Guertin D., Jacobson N., Tankala K., Galvanauskas A. *Conf. on Lasers and Electro-Optics/ Quantum Electronics and Laser Science and Photonic Applications Systems Technologies*, OSA Technical Digest Series (CD) (New York: Optical Society of America, 2007) paper CTuBB3.
11. Gaponov D.A., Février S., Devautour M., Roy P., Likhachev M.E., Aleshkina S.S., Salganskii M.Y., Yashkov M.V., Guryanov A.N. *Opt. Lett*., **35**, 2233 (2010).
12. Daniault L., Gaponov D.A., Hanna M., Février S., Roy P., Druon F., Georges P., Likhachev M.E., Salganskii M.Y., Yashkov M.V. *Appl. Phys. B*, **103**, 615 (2011).
13. Filippov V., Chamorovskii Yu., Kerttula J., Golant K., Pessa M., Okhotnikov O.G. *Opt. Express*, **16**, 1929 (2008).
14. Trikshev A.I., Kurkov A.S., Tsvetkov V.B., Filatova S.A., Kertulla J., Filippov V., Chamorovskiy Yu.K., Okhotnikov O.G. *Laser Phys. Lett.*, **10**, 065101 (2013).
15. Stacey C.D., Jenkins R.M., Banerji J., Davies A.R. *Opt. Commun*., **269**, 310 (2007).
16. Jung Y., Jeong Y., Brambilla G., Richardson D.J. *Opt. Lett*., **34** (15), 2369 (2009).
17. DiGiovanni D.J., MacChesney J.B., Kometani T.Y. *J. Non-Cryst. Solids*, **113**, 58 (1989).
18. Likhachev M.E., Bubnov M.M., Zotov K.V., Lipatov D.S., Yashkov M.V., Guryanov A.N. *Opt. Lett*., **34**, 3355 (2009).
19. Likhachev M., Aleshkina S., Shubin A., Bubnov M., Dianov E., Lipatov D., Guryanov A. *CLEO/Europe-EQEC 2011* (Munich, Germany, 2011) paper CJ.P.24.
20. Vukovic N., Broderick N.G., Petrovich M., Brambilla G., *IEEE Photonics Technol. Lett*., **20**, 1264 (2008).
21. Bogatyrev V.A., Bubnov M.M., Dianov E.M., Kurkov A.S., Mamyshev P.V., Prokhorov A.M., Rumyantsev S.D., Semenov V.A., Semenov S.L., Sysoliatin A.A., Chernikov S.V., Gur'yanov A.N., Devyatykh G.G., Miroshnichenko S.I. *J. Lightwave Technol.*, **9**, 561 (1991).
22. Bogatyrjov V.A., Sysoliatin A.A. *Proc. SPIE Int. Soc. Opt. Eng.*, **4204**, 274 (2001).
23. Andrianov A., Anashkina E., Muravyev S., Kim A. *Opt. Lett.*, **35**, 3805 (2010).
24. Tu H., Lægsgaard J., Zhang R., Tong S., Liu Y., Boppart S.A. *Opt. Express*, **21**, 23188 (2013).
25. Andrianov A.V., Anashkina E.A., Muravyev S.V., Kim A.V. *Kvantovaya Elektron*., **43**, 256 (2013) [*Quantum Electron*., **43**, 256 (2013)].
26. Anashkina E.A., Andrianov A.V., Akhmedzhanov R.A., Ilyakov I.E., Kim A.V., Mironov V.A., Muravyev S.V., Suvorov E.V., Tokman M.D., Fadeev D.A., Shishkin B.V. *Phys. Wave Phenom.*, **22**, 202 (2014).

27. Agrawal G.P. *Nonlinear Fiber Optics* (London: Elsevier, 2013).
28. Chi S., Chang C.W., Wen S. *Opt. Commun.*, **106**, 193 (1994).
29. Snyder A.W., Love J.D. *Optical Waveguide Theory* (London: Chapman and Hall, 1983; Moscow: Radio i Svyaz', 1987).
30. Andrianov A., Anashkina E., Kim A., Meyerov I., Lebedev S., Sergeev A., Mourou G. *Opt. Express*, **22**, 28256 (2014).